Journal of Materials Chemistry B

ROYAL SOCIETY OF CHEMISTRY

PAPER

View Article Online
View Journal | View Issue

Cite this: J. Mater. Chem. B, 2020, 8, 1906

Reactive oxygen species (ROS)-responsive ferrocene-polymer-based nanoparticles for controlled release of drugs†

Yoonhee Na,[ab] Jin Sil Lee,[ac] Jiseob Woo,[ab] Sukyung Ahn,[d] Eunhye Lee,[d] Won Il Choi *[a] and Daekyung Sung *[a]

Received 10th November 2019,
Accepted 29th January 2020

DOI: 10.1039/c9tb02533b

rsc.li/materials-b

Ferrocene-containing nanoparticles show reversible redox activity that could trigger drug release mediated by reactive oxygen species (ROS). In this study, four ferrocene-containing polymers, comprising ferrocenylmethyl methacrylate (FMMA)–methacrylic acid (MA) random copolymers, *i.e.*, poly(FMMA-*r*-MA), were synthesized *via* radical polymerization, resulting in self-assembled ferrocene nanoparticles (FNPs) with outstanding performance in environments in which ROS are present. These spherical FNPs have tunable diameters ranging from 270 nm to 180 nm and surface charges from −20 mV to −50 mV. Importantly, the diameters and surface charges of the FNPs changed dramatically after 2 h of post-treatment using 0.4 M hydrogen peroxide (H_2O_2) as the oxidant, indicating that the FNPs were highly ROS-sensitive. Furthermore, the controlled release of a model drug from the FNPs, reflected in the release profiles, indicates that these novel FNPs could be potentially used as drug carriers for the effective therapy of ROS-related diseases such as cancer and inflammation.

Introduction

Stimuli-responsive polymeric nanoparticles have attracted significant attention in the biomedical field for efficient drug delivery into target sites.[1] The physicochemical properties of polymeric nanoparticles could be dramatically changed by various stimuli such as pH,[2,3] light,[4–6] temperature,[7,8] ultrasound,[9] enzymes,[10,11] electricity,[12] solvents,[13] CO_2,[14] and redox reactions,[15–18] followed by controlled drug release under specific conditions. Among them, nanoparticles responsive to reactive oxygen species (ROS) as a result of redox stimuli are an ideal carrier because they could be used for the timely release of drugs in specific physiological environments. Endogenous ROS including hydrogen peroxide (H_2O_2), superoxide (O_2^-), hydroxyl radicals ($^{\bullet}OH$) or hypochlorite ions (OCl^-) perform important functions in intercellular signaling and biological metabolism.[19–21] In the case of a normal metabolism, the endogenous levels of ROS are low ($\sim 20 \times 10^{-9}$ M) but the level dramatically increases up to 100×10^{-6} M for an abnormal metabolism, including that associated with various diseases such as cancer and inflammation.[21–23] Therefore, increased levels of ROS in pathological regions could enable the controlled release of a drug at the target site using ROS-responsive polymeric nanoparticles.

ROS-responsive nanoparticles have been developed using various materials including thioethers, selenium/tellurium, thioketals, boronic esters, sulfides, and ferrocene groups.[24] Among them, ferrocene, an organometallic compound, has many advantages including uniquely reversible redox activity, stability, and a convenient synthesis process.[25–27] In addition, the hydrophobic neutral ferrocene molecule can be changed to the hydrophilic ferrocenium cation after oxidation without any change to its molecular structure and trigger ROS-mediated drug release *via* a hydrophobic-to-hydrophilic transition.[19] Thus, ferrocene-containing polymer nanoparticles could be potential carriers for effective ROS-responsive drug delivery.[28–30] Recently, Zhang *et al.* reported that redox-responsive ferrocene-containing amphiphilic PEG-*b*-PMAEFc block copolymers synthesized *via* atom transfer radical polymerization could self-assemble into nanoparticles for controlled release of rhodamine B in the presence of an oxidant.[16] Crespy *et al.* also developed functional nanocapsules composed of a PVFc-*b*-PMMA block copolymer for the efficient redox-responsive release of a hydrophobic drug *via* oxidation stimulation.[31] However, the aforementioned ferrocene-containing

[a] Center for Convergence Bioceramic Materials, Convergence R&D Division, Korea Institute of Ceramic Engineering and Technology, 202, Osongsaengmyeong 1-ro, Osong-eup, Heungdeok-gu, Cheongju, Chungbuk 28160, Republic of Korea. E-mail: choi830509@kicet.re.kr, dksung@kicet.re.kr; Fax: +82-43-913-1597; Tel: +82-43-913-1513, +82-43-913-1511
[b] School of Chemical & Biomolecular Engineering, Yonsei University, 50 Yonsei Ro, Seodaemun Gu, Seoul, 03722, Republic of Korea
[c] School of Materials Science and Engineering, Gwangju Institute of Science and Technology, 123 Cheomdan-gwagiro, Buk-gu, Gwangju 61005, Republic of Korea
[d] Utah-Inha DDS and Advanced Therapeutics Research Center, 3F, Venture-ro 100beon-gil, Yeonsu-gu, Incheon, 22013, Republic of Korea

† Electronic supplementary information (ESI) available. See DOI: 10.1039/c9tb02533b

polymers and nanoparticles have various disadvantages that limit their application in drug delivery.[32,33] The polymer is obtained in low yields because the synthesis procedure consists of multistep processes, the ferrocene-containing nanoparticles are poorly soluble and have poor stability, and the size and surface charges of these nanoparticles are uncontrollable. Moreover, the development of ROS-sensitive nanoparticles from these ferrocene-containing polymers for efficient drug delivery has not yet been reported.

This prompted us to synthesize four ferrocene-containing polymers in the form of ferrocenylmethyl methacrylate (FMMA)–methacrylic acid (MA) random copolymers, *i.e.*, (poly(FMMA-*r*-MA)). The polymers were prepared by using simple radical polymerization by varying the molar ratios of FMMA and MA in a one-step synthesis with a favorable yield. In addition, novel ferrocene nanoparticles (FNPs), characterized by improved stability and high ROS sensitivity, were simply prepared using the different poly(FMMA-*r*-MA) copolymers *via* nanoprecipitation and optimized for stable drug delivery. The purity and molecular weight of the synthesized ferrocene-containing polymers were determined by proton nuclear magnetic resonance (^{1}H NMR) spectroscopy and gel permeation chromatography (GPC), respectively. The physicochemical properties of the FNPs were characterized by dynamic light scattering (DLS) and transmission electron microscopy (TEM). The stability of the FNPs was evaluated in biological buffers and during resuspension after freeze-drying without using any cryoprotectants, by monitoring the changes in the appearance and diameter of the nanoparticles. Furthermore, the ROS-responsive properties of the FNPs were analyzed using hydrogen peroxide (H_2O_2) as the oxidant, and finally, controlled drug release was assessed upon application of ROS stimuli.

Materials and methods

Materials

FMMA (95%), MA (99%), tetrahydrofuran (THF, anhydrous, 99.9%) and an inhibitor-removal column were purchased from Sigma-Aldrich (St. Louis, MO, USA). 2,2-Azobisisobutyronitrile (AIBN, 99%) was obtained from Daejung (Seoul, Korea). Deionized (DI) water and phosphate buffered saline (PBS, pH 7.4) were purchased from HyClone (Logan, UT, USA). Hydrogen peroxide (H_2O_2, 30%) was obtained from Junsei Chemical Co. (Tokyo, Japan). Nile red was purchased from Sigma-Aldrich (St. Louis, MO, USA). For *in vitro* cell culture, Dulbecco's modified Eagle's medium (DMEM), fetal bovine serum (FBS), and antibiotic–antimycotic (AA) solution were obtained from Gibco (Grand Island, NY, USA). Cell Counting Kit-8 (CCK-8) was purchased from Dojindo Laboratories (Kumamoto, Japan). All solvents were used as received without any further purification.

Synthesis of ferrocene-containing polymers (poly(FMMA-*r*-MA))

The ferrocene-containing polymers were simply synthesized *via* radical polymerization, as previously reported.[34,35] Prior to polymerization, MA was passed through the inhibitor-removal column for 2 h to remove inhibitors that could result in poor polymerization. FMMA (0.4 mmol) and MA (0.5 mmol) were dissolved in 2 mL of anhydrous THF and then AIBN (0.12 mmol) was added as the radical initiator, followed by degassing (Ar gas bubbling for 5 min), after which the reaction mixture was sealed with a Teflon film. Next, the polymerization reaction was carried out at 70 °C for 24 h while stirring and the final product was cooled to below 25 °C and finally stored at 4 °C before use. Four ferrocene-containing polymers including Poly C0.5 [0.4 : 0.5], Poly C1 [0.4 : 1], Poly C2 [0.4 : 2], and Poly C3 [0.4 : 3] were easily prepared by varying the initial molar ratios of the FMMA and MA monomers. The purities of these ferrocene-containing polymers were analyzed *via* ^{1}H NMR (400 MHz, JEOL JNM-ECZ400S/L1). The polymers were dissolved in deuterochloroform ($CDCl_3$) at 25 °C and identified as poly(FMMA-*r*-MA) with δ = 4.8 (br, 2H, CO_2–CH_2 of FMMA), 4.4–4.1 (br, 9H of FMMA), 3.7–3.3 (br, 20H), 2.7–2.5 (br, 18H), 2.0–1.7 (br, 15H), and 1.1–0.8 (br, 17H) ppm. In addition, the molecular weight (M_w) and polydispersity index (PDI = M_w/M_n) of the polymers were measured using GPC (Agilent 1200S/miniDAWN TREOS) with THF as the eluent at a flow rate of 1.0 mL min^{-1} at 35 °C.

Preparation of the FNPs

The FNPs were prepared by employing a simple nanoprecipitation method with additional modification, as previously reported.[36] First, the ferrocene-containing polymers (5 mg) were dissolved in 1 mL of THF at room temperature (25 °C). Next, the solution containing the polymer was added dropwise to 5 mL of de-ionized water while stirring gently using a syringe pump (LEGATO100, Kd Scientific, Korea) with a flow rate of 0.075 mL s^{-1}. Subsequently, the mixture was stirred for 5 min at 25 °C to stabilize the newly formed nanoparticles and the THF solvent was completely removed by vacuum drying for 2 h. The physicochemical properties, *i.e.*, the size, dispersity, and surface charge, of the FNPs were analyzed by using DLS on a Zetasizer instrument (ZEN3600, Malvern, Worcestershire, UK). In addition, the morphologies of the FNPs were obtained at 25 °C by employing TEM (JEM-2100PlusHR, JEOL, Tokyo, Japan). TEM observations were performed by dropping the nanoparticle solution onto a carbon-coated copper grid without using staining and then drying for 3 d at room temperature.

Stability analysis of the FNPs

The stability of the FNPs was analyzed as a function of time under three different conditions. The appearance and hydrodynamic diameters of the FNPs (1 mg mL^{-1}) were measured using DLS at each time point for four weeks in an aqueous solution (de-ionized water, 1st condition) and at selected time points (1, 3, 5, and 7 d) in biological buffer (PBS, 2nd condition) using a shaking incubator at 100 rpm and 37 °C. Finally, the re-dispersity of the freeze-dried FNPs was assessed without using any cryoprotectants such as trehalose, sucrose, or glucose after resuspension in biological buffer at a concentration of 1 mg mL^{-1} (3rd condition).

Characterization of the ROS-responsive properties of the FNPs

To analyze the ROS-sensitive behavior of the FNPs, 0.4 M of hydrogen peroxide (H_2O_2) as the oxidizing agent was added to an aqueous solution containing FNPs (1 mg mL^{-1}) while stirring gently. Then, the changes in the size and surface charges of the nanoparticles due to oxidation were monitored at each time point (0 h, 1 h, 2 h, 4 h, and 24 h) using the Zetasizer instrument. Furthermore, the morphological changes and appearance of the oxidized FNPs were analyzed at selected time points (0 h, 2 h, and 4 h) using TEM and a digital camera, respectively.

ROS-responsive release profiles of drugs from the FNPs

The ROS-responsive patterns of drugs released from the FNPs were evaluated by utilizing a lipophilic fluorescent probe (Nile red) as the model drug. Nile red (100 μg mL^{-1} in THF) was mixed with 5 mg of the ferrocene-containing polymer and the reaction was allowed to proceed under rotary shaking for 1 h at room temperature. Next, the mixture was added dropwise to 5 mL de-ionized water under gentle stirring using a syringe pump, following which the THF solvent was removed by vacuum drying, as described above. Finally, the Nile red not loaded into FNP(C2) was removed by ultrafiltration using Amicon Ultra-15 centrifugal filters (a molecular weight cut-off (MWCO) of 100 kDa) at 3000 rpm for 5 min. The loading content (LC) and loading efficiency (LE) of the drug into the FNPs were determined by measuring the unloaded Nile red using a microplate reader (TECAN, Männedorf, Switzerland) at an excitation wavelength of 530 nm and emission wavelength of 570 nm. The values of the LC and LE were calculated using the following equations, as previously reported.[37–39]

$$\mathrm{LC} = \frac{\text{weight of fed drugs} - \text{weight of unloaded drugs}}{\text{weight of FNP}} \times 100$$

$$\mathrm{LE} = \frac{\text{weight of fed drugs} - \text{weight of unloaded drugs}}{\text{weight of fed drugs}} \times 100$$

The solution of FNP(C2) loaded with Nile red (1 mg mL^{-1}) was fed into a Float-A-Lyzer G2 dialysis device with an MWCO of 100 kDa (Spectra/Pro Dialysis membrane, Repligen, Massachusetts, USA). Then, the release device was immersed in 10 mL of PBS containing 0.4 M H_2O_2 in a shaking incubator at 100 rpm and 37 °C. The released medium was collected at selected time points for 72 h and measured using the microplate reader (ex. 530 nm/em. 570 nm).

In vitro cytotoxicity of the FNPs

The cytotoxicity of the FNPs was determined by using the CCK-8 assay. Mouse fibroblast cells (NIH 3T3, from ATCC) were seeded into a 96-well cell culture plate with 10 000 cells per well and incubated overnight at 37 °C under a 5% CO_2 atmosphere. Then, the cells were treated with various concentrations (10, 20, 50, and 100 μg mL^{-1}) of the FNP(C2) and further incubated for 24 h. Finally, the CCK-8 kit solution, diluted 10 times, was added to each well and the cell medium was detected after 1 h post-treatment at 37 °C using the microplate reader at a wavelength of 450 nm, as previously reported.[40,41] All the experiments were performed in triplicate.

Results and discussion

Synthesis and characterization of the ferrocene-containing polymers (poly(FMMA-*r*-MA))

Among the various organometallic polymers, ferrocene-containing polymers are highly promising materials for drug delivery carriers owing to their high redox characteristics, excellent structural stability, and low biotoxicity.[42] However, as the ferrocene group is poorly soluble in aqueous solutions, the copolymerization of hydrophilic moieties such as carboxylic acids, amines, and PEG with ferrocene units is necessary to form self-assembled nanostructures. In this study, we developed a facile method, based on radical polymerization using AIBN as the radical initiator, to synthesize ROS-responsive, amphiphilic ferrocene polymers (poly(FMMA-*r*-MA)). The polymers are composed of an FMMA monomer with a hydrophobic ferrocene moiety and an MA monomer with a hydrophilic COOH group. As shown in Fig. 1a, the density of the hydrophobic ferrocene and hydrophilic COOH residues in the ferrocene-containing polymers can be controlled by simply changing the initial molar ratios of FMMA and MA. Using this approach, we successfully synthesized four ferrocene-containing polymers (Poly C0.5, C1, C2, and C3).

The purity of the synthesized ferrocene-containing polymers was determined by analyzing the typical peaks of the methacrylate protons of the FMMA and MA monomers at 5.58 and 6.15 ppm in the ^{1}H NMR spectrum. After polymerization, the peaks of the monomeric precursors of all the polymeric groups in the ferrocene-containing polymers completely disappeared

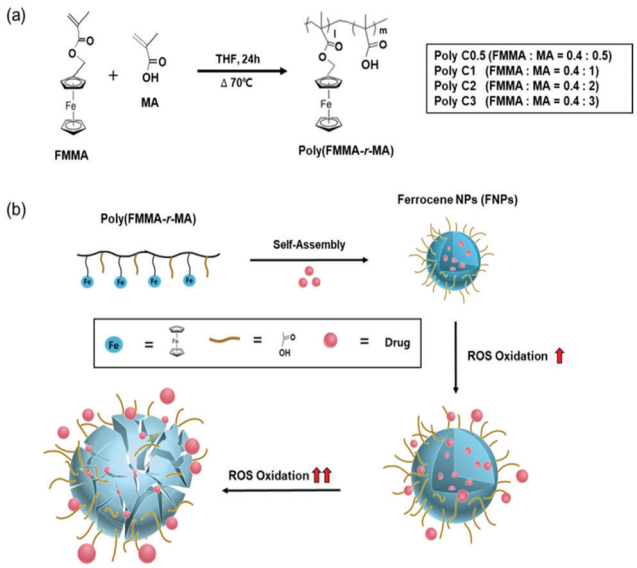

Fig. 1 Schematics showing (a) synthesis of ferrocene-containing polymers (poly(FMMA-*r*-MA)), referred to as Poly C0.5, Poly C1, Poly C2, and Poly C3, formed by varying the molar ratios of FMMA and MA monomers and (b) preparation of ferrocene-containing nanoparticles (FNPs) for the ROS-responsive release of a model drug.

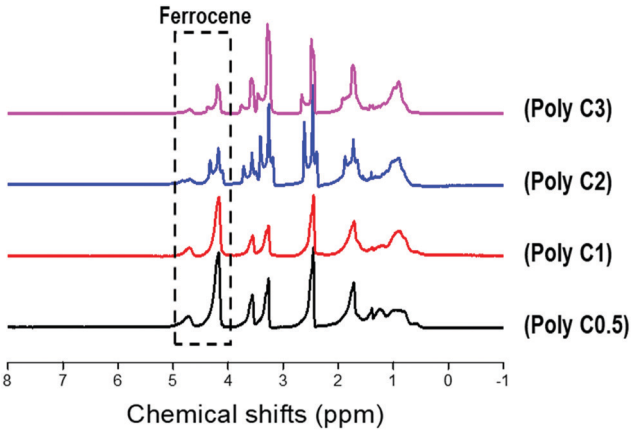

Fig. 2 ^{1}H NMR spectra of the ferrocene-containing polymers (Poly C0.5, Poly C1, Poly C2, and Poly C3) exhibiting the ferrocene peaks. This enables the actual ferrocene content of the different polymers to be compared.

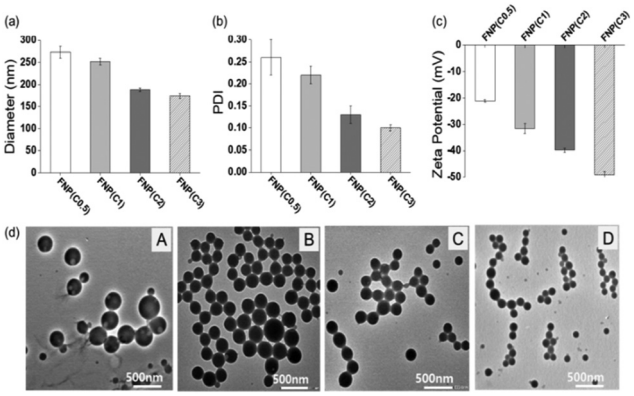

Fig. 3 (a) Hydrodynamic diameters, (b) polydispersity index (PDI), (c) surface charges and (d) TEM images of the ferrocene-containing nanoparticles (A: FNP(C0.5), B: FNP(C1), C: FNP(C2), and D: FNP(C3), scale bar: 500 nm).

and the broad peaks of the alkyl chains of the polymers became clearly visible, indicating that the four ferrocene-containing polymers were successfully synthesized without any impurity (Fig. 2). Interestingly, the intensity of the new peak in the range 4.1 to 4.8 ppm, which corresponds to the protons of the ferrocene unit in the ferrocene-containing polymers, gradually decreased as the ratio of MA increased from Poly C0.5 to Poly C3. This implies that the compositions of the ferrocene-containing polymers were such that the initial molar ratios of the monomers were nearly maintained. In addition, the molecular weight and PDI of the ferrocene-containing polymers were evaluated *via* GPC, and the results are presented in Table 1 and Fig. S1 (ESI†). The molecular weights of the ferrocene polymers ranging from 4 kDa to 10 kDa showed an increasing trend as the proportion of MA increased from Poly C0.5 to Poly C3. The fact that the PDI was less than 2 indicated that the molecular weight distribution was acceptable. This suggested that the polymerization step led to the successful synthesis of monodisperse ferrocene-containing polymers. The yields of the ferrocene-containing polymers were 97.3% (Poly C0.5), 95.1% (Poly C1), 99.7% (Poly C2), and 98.1% (Poly C3) (Table S1, ESI†).

Preparation and characterization of FNPs

FNPs, designated as FNP(C0.5), FNP(C1), FNP(C2), and FNP(C3), were spontaneously prepared using the synthesized ferrocene-containing polymers, which could self-assemble into stable nanoaggregates in aqueous solutions with a hydrophobic core comprising ferrocene and a hydrophilic shell comprising the carboxyl groups. As shown in Fig. 3, the hydrodynamic diameter, PDI, and surface charges of the FNPs could be controlled by varying the ratio of FMMA to MA in the ferrocene-containing polymers. The size of the FNPs decreased from 273 nm to 174 nm as the number of hydrophilic carboxyl groups increased from FNP(C0.5) to FNP(C3). Likewise, the surface charges of the FNPs became highly negative, ranging from −21 to −49 mV upon increasing the number of carboxyl groups. In addition, the particle size distribution of the FNPs was acceptable at a PDI below 0.2, indicating that the FNPs could effectively undergo self-assembly owing to the proper hydrophilic/hydrophobic balance in the amphiphilic ferrocene-containing polymers. Furthermore, morphological studies of all the FNPs indicated spherical shapes and the diameters of the FNPs observed *via* TEM (FNP(0.5) – 250 nm, FNP(C1) – 208 nm, FNP(C2) – 164 nm, and FNP(C3) – 111 nm) were slightly smaller than those measured *via* DLS (Table S2, ESI†).

This is because the FNPs observed using TEM could have shrunk and become dehydrated during the freeze-drying process (Fig. 3d).

Table 1 GPC results of the synthesized ferrocene-containing polymers (poly(FMMA-*r*-MA): Poly C0.5, Poly C1, Poly C2, and Poly C3). The molecular weights (M_w) and polydispersity index (PDI) of the polymers were analyzed using a standard polystyrene sample

Polymer groups	M_n (g mol^{-1})	M_w (g mol^{-1})	PDI
Poly C0.5	2376	4419	1.860
Poly C1	3905	5942	1.521
Poly C2	4027	8020	1.991
Poly C3	4821	10 493	2.177

Stability analysis of the FNPs

The stability of nanoparticles is an important factor for their potential use in various biomedical applications. The stability of the FNPs was assessed by using DLS to monitor the changes in their diameter and appearance under three different conditions (Fig. 4). In aqueous solution, the hydrodynamic diameters of the FNPs were analyzed in de-ionized water for four weeks at 37 °C and 100 rpm. No obvious variation in size was observed for FNP(C1), FNP(C2), and FNP(C3) during this time; however, the size of FNP(C0.5) rapidly increased, producing partial aggregation in a week, indicating the instability of these nanoparticles. Next, the stability of the FNPs was monitored in biological buffer (PBS). FNP(C2) and FNP(C3) did not aggregate even after a week, whereas FNP(C1) showed signs of aggregation, suggesting that FNP(C2) and FNP(C3) have high stability owing to their highly negative charges.[43] More importantly, the stability of

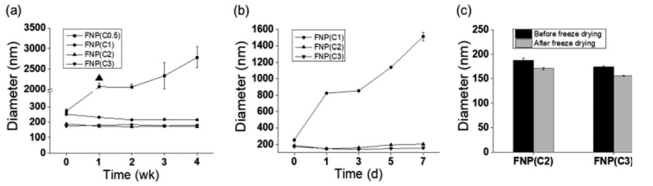

Fig. 4 Stability analysis of the ferrocene-containing nanoparticles in (a) aqueous solution and (b) biological buffer at 100 rpm and 37 °C. (c) Size change of the ferrocene-containing nanoparticles re-dispersed in PBS (pH 7.4) after lyophilization without any cryoprotectants. In the case of FNP(C0.5), the symbol (▲) denotes partial aggregation of the nanoparticles.

the FNPs was assessed during resuspension without adding any cryoprotectants such as trehalose, sucrose, or glucose. Freeze-dried FNP(C2) and FNP(C3) were readily re-dispersed in the biological buffer without any critical diameter changes, implying that FNP(C2) and FNP(C3) have excellent stability and could serve as potential platforms for effective *in vivo* drug delivery.

ROS-responsiveness of the FNPs

The ROS sensitivity of the FNPs including FNP(C1), FNP(C2), and FNP(C3) was analyzed in terms of the changes in their size, surface charge, and morphology using 0.4 M H_2O_2 as a water-soluble oxidant (Fig. 5). After treatment with the oxidant, the diameters of the FNPs in all groups dramatically increased with increasing incubation time because H_2O_2 can rapidly diffuse across the carboxyl shell of the nanoparticles and oxidize the groups attached to the ferrocene core.[16,44,45] In particular, FNP(C1) and FNP(C2) showed much higher ROS-responsiveness by increasing their size to above 1000 nm even during the 2 h post-treatment compared to FNP(C3), indicating that the nanoparticles with relatively fewer carboxyl groups could be more sensitive in ROS environments. In addition, the surface charge of FNP(C1) and FNP(C2) significantly decreased compared to that of FNP(C3), suggesting that the formation of positively charged ferrocenium ions (Fe^{3+}) from the ferrocene groups in the FNPs could reduce the negative surface charges of the nanoparticles.

TEM was used to visualize the redox-sensitive behavior of the FNPs before and after oxidation of the nanoparticles. Among the FNPs, FNP(C2), characterized by high stability and good ROS-responsiveness, was further analyzed. The size of these FNPs increased from approximately 920 nm in 2 h to approximately 2900 nm in 4 h and they disintegrated into fragments after 4 h of treatment with H_2O_2. These results indicate that these novel FNPs could be used as smart ROS-sensitive carriers for efficient drug delivery into target sites.

In vitro drug release and cytotoxicity of ROS-sensitive FNPs

To verify the ROS-responsive release profile of the FNPs, Nile red was specifically chosen as the hydrophobic model drug and loaded into FNP(C2) because it does not experience any fluorescence quenching in H_2O_2 for 72 h.[46,47] The FNPs showed an LC of 1.9 wt% and LE of 99% and their physicochemical characteristics (size, PDI, and surface charge) remained unmodified after the hydrophobic drug was loaded (Fig. S2, ESI†). As shown in Fig. 6, the pattern followed when Nile red was released from FNP(C2) significantly differed in the presence and absence of the oxidant (0.4 M H_2O_2). In the absence of the oxidant, the amount of Nile red released from the nanoparticles was approximately 8% at 8 h owing to only the effect of diffusion from the stable nanoparticles without H_2O_2.[16,18] In contrast, the amount of drug released from the nanoparticles in the presence of 0.4 M H_2O_2 dramatically increased to approximately 25% (three times higher) at 8 h, indicating that the release rate of the model drug could be clearly controlled by the FNPs under ROS conditions. The FNPs might be swollen and even broken by the immediate disappearance of the π–π stacking effect because of the electrostatic repulsion between the ferrocinium (Fe^{3+}) ions in the oxidized ferrocene core.[18,31,48,49] Therefore, a larger diffusion space and channel in the swollen FNPs could cause rapid release of the encapsulated Nile red.[16,18,48]

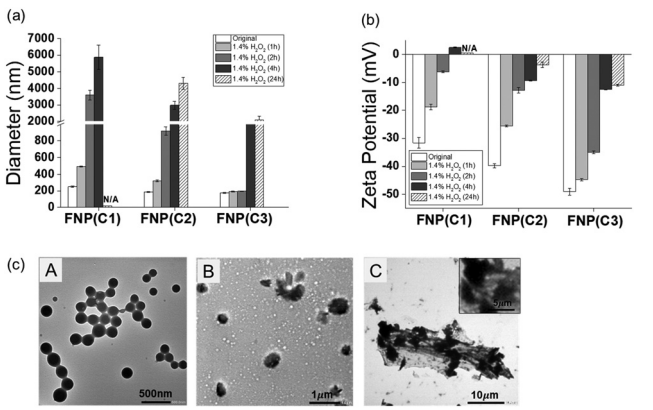

Fig. 5 Characterization of the ROS-responsive properties of the ferrocene-containing nanoparticles: (a) hydrodynamic diameters, (b) surface charges, and (c) TEM images of the FNPs after oxidation using 0.4 M H_2O_2. (A: FNP(C2) before oxidation, B: FNP(C2) 2 h post-oxidation, and C: FNP(C2) 4 h post-oxidation).

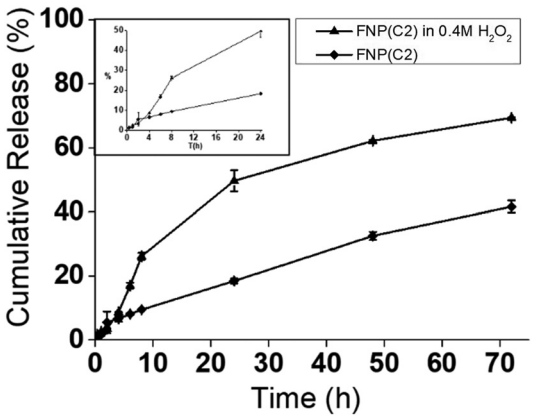

Fig. 6 Release profiles of Nile red from ferrocene-containing nanoparticles (FNP (C2)) in PBS (pH 7.4) containing 0.4 M H_2O_2 at 100 rpm and 37 °C. The fluorescence intensity of the oxidized nanoparticles increased with time, measured by a microplate reader in fluorescence detection mode (ex. 520 nm/em. 575 nm).

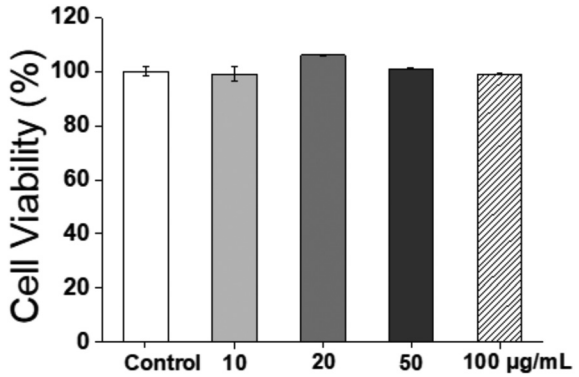

Fig. 7 *In vitro* cytotoxicity of the ferrocene-containing nanoparticles (FNP(C2)) ranging from 10 to 100 μg mL^{-1} in NIH 3T3 fibroblast cells. The cytotoxicity was measured using the CCK-8 assay. Values on the graph are expressed as means ± standard deviations of three experimental measurements.

In addition, the cytotoxicity of FNP(C2) was assessed using NIH 3T3 fibroblast cells to verify the biocompatibility of the nanoparticles for various biomedical applications. As shown in Fig. 7, a cell viability in excess of 95% was measured in nanoparticle concentrations ranging from 0 to 100 μg mL^{-1}, implying that the ROS-responsive FNP(C2) with favorable biocompatibility could be suitable for targeted and controlled drug release for treating ROS-related diseases.

Conclusion

Novel amphiphilic ferrocene-containing polymers, poly(FMMA-*r*-MA) random copolymers, were successfully synthesized *via* simple radical polymerization. This approach has the following advantages: a simple one-step synthesis process with high yield together with increased stability, and, furthermore, the FNPs fabricated by using this method are highly sensitive to ROS. The physicochemical properties of the FNPs were optimized by using poly(FMMA-*r*-MA) random copolymers with different monomer ratios under mild nanoprecipitation conditions. Among the FNPs, FNP(C2) and FNP(C3) showed high stability in aqueous solutions and biological buffer and even during resuspension after lyophilization without using any cryoprotectants. In addition, the ROS-responsiveness of the FNPs resulted in the controlled release of a model hydrophobic drug upon oxidation with H_2O_2; this property of the FNPs may play a more important role in the specific physiological environment of a disease than in normal tissues. These results indicated that the stability, ROS-responsiveness, and biocompatibility of these FNPs make them suitable for use in various biomedical applications, especially for cancer and inflammation treatment.

Conflicts of interest

There are no conflicts to declare.

Acknowledgements

This research was supported by the National Research Foundation of Korea (NRF) funded by the Korea government (MSIT) (grant No. NRF-2018R1D1A1B07043620) and a grant of the Korea Institute of Ceramic Engineering and Technology (KICET).

References

1 Y. Huang, Q. Chen, P. Ma, H. Song, X. Ma, Y. Ma, X. Zhou, S. Gou, Z. Xu, J. Chen and B. Xiao, Facile Fabrication of Oxidation-Responsive Polymeric Nanoparticles for Effective Anticancer Drug Delivery, *Mol. Pharmaceutics*, 2019, **16**, 49–59.
2 W. Gao, J. M. Chan and O. C. Farokhzad, pH-responsive nanoparticles for drug delivery, *Mol. Pharmaceutics*, 2010, **7**, 1913–1920.
3 K. S. Soppimath, D. C. W. Tan and Y. Y. Yang, pH-Triggered Thermally Responsive Polymer Core-Shell Nanoparticles for Drug Delivery, *Adv. Mater.*, 2005, **17**, 318–323.
4 H. Kang, A. C. Trondoli, G. Zhu, Y. Chen, Y.-J. Chang, H. Liu, Y.-F. Huang, X. Zhang and W. Tan, Near-infrared light-responsive core–shell nanogels for targeted drug delivery, *ACS Nano*, 2011, **5**, 5094–5099.
5 C. Alvarez-Lorenzo, L. Bromberg and A. Concheiro, Light-sensitive intelligent drug delivery systems, *Photochem. Photobiol.*, 2009, **85**, 848–860.
6 N. C. Fan, F. Y. Cheng, J. A. Ho and C. S. Yeh, Photocontrolled targeted drug delivery: photocaged biologically active folic acid as a light-responsive tumor-targeting molecule, *Angew. Chem., Int. Ed.*, 2012, **51**, 1–6.
7 S. R. Sershen, S. L. Westcott, N. J. Halas and J. L. West, Temperature-sensitive polymer–nanoshell composites for photothermally modulated drug delivery, *J. Biomed. Mater. Res.*, 2000, **51**, 293–298.
8 S. Chen, Y. Li, C. Guo, J. Wang, J. Ma, X. Liang, L.-R. Yang and H.-Z. Liu, Temperature-responsive magnetite/PEO–PPO–PEO block copolymer nanoparticles for controlled drug targeting delivery, *Langmuir*, 2007, **23**, 12669–12676.
9 J. L. Paris, M. V. Cabañas, M. Manzano and M. Vallet-Regi, Polymer-Grafted Mesoporous Silica Nanoparticles as Ultrasound-Responsive Drug Carriers, *ACS Nano*, 2015, **9**, 11023–11033.
10 Q. Hu, P. S. Katti and Z. Gu, Enzyme-responsive nanomaterials for controlled drug delivery, *Nanoscale*, 2014, **6**, 12273–12286.
11 R. de la Rica, D. Aili and M. M. Stevens, Enzyme-responsive nanoparticles for drug release and diagnostics, *Adv. Drug Delivery Rev.*, 2012, **64**, 967–978.
12 J. Ge, E. Neofytou, T. J. Cahill III, R. E. Beygui and R. N. Zare, Drug release from electric-field-responsive nanoparticles, *ACS Nano*, 2011, **6**, 227–233.
13 J. Dong and J. Zhou, Solvent-responsive behavior of polymer-brush-modified amphiphilic gold nanoparticles, *Macromol. Theory Simul.*, 2013, **22**, 174–186.
14 H. Che, M. Huo, L. Peng, Q. Ye, J. Guo, K. Wang, Y. Wei and J. Yuan, CO_2-switchable drug release from magneto-polymeric nanohybrids, *Polym. Chem.*, 2015, **6**, 2319–2326.

15 M. Huo, J. Yuan, L. Tao and Y. Wei, Redox-responsive polymers for drug delivery: from molecular design to applications, *Polym. Chem.*, 2014, **5**, 1519–1528.
16 L. Liu, L. Rui, Y. Gao and W. Zhang, Self-assembly and disassembly of a redox-responsive ferrocene-containing amphiphilic block copolymer for controlled release, *Polym. Chem.*, 2015, **6**, 1817–1829.
17 J. H. Ryu, R. Roy, J. Ventura and S. Thayumanavan, Redox-sensitive disassembly of amphiphilic copolymer based micelles, *Langmuir*, 2010, **26**, 7086–7092.
18 Y. Wang, Y.-L. Luo, F. Xu, Y.-S. Chen and W. Tang, Redox-responsive PAEFc-*b*-PDMAEMA amphiphilic block copolymer self-assembly micelles: Physicochemical properties and anticancer drug controlled release, *J. Ind. Eng. Chem.*, 2017, **48**, 66–78.
19 G. Saravanakumar, J. Kim and W. J. Kim, Reactive-Oxygen-Species-Responsive Drug Delivery Systems: Promises and Challenges, *Adv. Sci.*, 2017, **4**, 1600124.
20 S. H. Lee, M. K. Gupta, J. B. Bang, H. Bae and H. J. Sung, Current progress in Reactive Oxygen Species (ROS)-Responsive materials for biomedical applications, *Adv. Healthcare Mater.*, 2013, **2**, 908–915.
21 H. Ye, Y. Zhou, X. Liu, Y. Chen, S. Duan, R. Zhu, Y. Liu and L. Yin, Recent Advances on Reactive Oxygen Species-Responsive Delivery and Diagnosis System, *Biomacromolecules*, 2019, **20**, 2441–2463.
22 B. Chance, H. Sies and A. Boveris, Hydroperoxide metabolism in mammalian organs, *Physiol. Rev.*, 1979, **59**, 527–605.
23 T. P. Szatrowski and C. F. Nathan, Production of large amounts of hydrogen peroxide by human tumor cells, *Cancer Res.*, 1991, **51**, 794–798.
24 V. Taresco, C. Alexander, N. Singh and A. K. Pearce, Stimuli-Responsive Prodrug Chemistries for Drug Delivery, *Adv. Chemother.*, 2018, **1**, 1800030.
25 M. F. Fouda, M. M. Abd-Elzaher, R. A. Abdelsamaia and A. A. Labib, On the medicinal chemistry of ferrocene, *Appl. Organomet. Chem.*, 2007, **21**, 613–625.
26 N. G. Connelly and W. E. Geiger, Chemical redox agents for organometallic chemistry, *Chem. Rev.*, 1996, **96**, 877–910.
27 G. Gasser, I. Ott and N. Metzler-Nolte, Organometallic anticancer compounds, *J. Med. Chem.*, 2010, **54**, 3–25.
28 C. Zuo, J. Peng, Y. Cong, X. Dai, X. Zhang, S. Zhao, X. Zhang and L. Ma, Fabrication of supramolecular star-shaped amphiphilic copolymers for ROS-triggered drug release, *J. Colloid Interface Sci.*, 2018, **514**, 122–131.
29 J. G. Zhang, X. Y. Zhang, H. Yu, Y. L. Luo, F. Xu and Y. S. Chen, Preparation, self-assembly and performance modulation of gold nanoparticles decorated ferrocene-containing hybrid block copolymer multifunctional materials, *J. Ind. Eng. Chem.*, 2018, **65**, 224–235.
30 S. Mu, Q. Ling, X. Liu, J. Ruiz, D. Astruc and H. Gu, Supramolecular redox-responsive substrate carriers activity of a ferrocenyl Janus device, *J. Inorg. Biochem.*, 2019, **193**, 31–41.
31 R. H. Staff, M. Gallei, M. Mazurowski, M. Rehahn, R. Berger, K. Landfester and D. Crespy, Patchy nanocapsules of poly (vinylferrocene)-based block copolymers for redox-responsive release, *ACS Nano*, 2012, **6**, 9042–9049.
32 S. Mu, W. Liu, Q. Ling, X. Liu and H. Gu, Ferrocenyl amphiphilic Janus dendrimers as redox-responsive micellar carriers, *Appl. Organomet. Chem.*, 2019, **33**, e4908.
33 G. Qiu, X. Liu, B. Wang, H. Gu and W. Wang, Ferrocene-containing Amphiphilic Polynorbornenes as Biocompatible Drug Carriers, *Polym. Chem.*, 2019, **10**, 2527–2539.
34 X. Wu, Y. Qiao, H. Yang and J. Wang, Self-assembly of a series of random copolymers bearing amphiphilic side chains, *J. Colloid Interface Sci.*, 2010, **349**, 560–564.
35 D. Sung and S. Yang, Facile method for constructing an effective electron transfer mediating layer using ferrocene-containing multifunctional redox copolymer, *Electrochim. Acta*, 2014, **133**, 40–48.
36 W. I. Choi, N. Kamaly, L. Riol-Blanco, I.-H. Lee, J. Wu, A. Swami, C. Vilos, B. Yameen, M. Yu, J. Shi and I. Tabas, A solvent-free thermosponge nanoparticle platform for efficient delivery of labile proteins, *Nano Lett.*, 2014, **14**, 6449–6455.
37 M. K. Gupta, T. A. Meyer, C. E. Nelson and C. L. Duvall, Poly (PS-*b*-DMA) micelles for reactive oxygen species triggered drug release, *J. Controlled Release*, 2012, **162**, 591–598.
38 X. Mei, D. Chen, N. Li, Q. Xu, J. Ge, H. Li and J. Lu, Hollow mesoporous silica nanoparticles conjugated with pH-sensitive amphiphilic diblock polymer for controlled drug release, *Microporous Mesoporous Mater.*, 2012, **152**, 16–24.
39 J. Yoo, N. S. Rejinold, D. Lee, S. Jon and Y.-C. Kim, Protease-activatable cell-penetrating peptide possessing ROS-triggered phase transition for enhanced cancer therapy, *J. Controlled Release*, 2017, **264**, 89–101.
40 Y. Li, L. Sun, M. Jin, Z. Du, X. Liu, C. Guo, Y. Li, P. Huang and Z. Sun, Size-dependent cytotoxicity of amorphous silica nanoparticles in human hepatoma HepG2 cells, *Toxicol. In Vitro*, 2011, **25**, 1343–1352.
41 Z.-H. Jiao, M. Li, Y.-X. Feng, J.-C. Shi, J. Zhang and B. Shao, Hormesis effects of silver nanoparticles at non-cytotoxic doses to human hepatoma cells, *PLoS One*, 2014, **9**, e102564.
42 F. Xu, H. Li, Y.-L. Luo and W. Tang, Redox-responsive self-assembly micelles from poly (n-acryloylmorpholine-*block*-2-acryloyloxyethyl ferrocenecarboxylate) amphiphilic block copolymers as drug release carriers, *ACS Appl. Mater. Interfaces*, 2017, **9**, 5181–5192.
43 G.-Y. Liou and P. Storz, Reactive oxygen species in cancer, *Free Radical Res.*, 2010, **44**, 479–496.
44 M. López-Lázaro, Dual role of hydrogen peroxide in cancer: possible relevance to cancer chemoprevention and therapy, *Cancer Lett.*, 2007, **252**, 1–8.
45 P. Prasad, C. R. Gordijo, A. Z. Abbasi, A. Maeda, A. Ip, A. M. Rauth, R. S. DaCosta and X. Y. Wu, Multifunctional albumin–MnO_2 nanoparticles modulate solid tumor microenvironment by attenuating hypoxia, acidosis, vascular endothelial growth factor and enhance radiation response, *ACS Nano*, 2014, **8**, 3202–3212.

46 L. Xu, M. Zhao, W. Gao, Y. Yang, J. Zhang, Y. Pu and B. He, Polymeric nanoparticles responsive to intracellular ROS for anticancer drug delivery, *Colloids Surf., B*, 2019, **181**, 252–260.
47 C. de Gracia Lux, S. Joshi-Barr, T. Nguyen, E. Mahmoud, E. Schopf, N. Fomina and A. Almutairi, Biocompatible polymeric nanoparticles degrade and release cargo in response to biologically relevant levels of hydrogen peroxide, *J. Am. Chem. Soc.*, 2012, **134**, 15758–15764.
48 Y. Xu, L. Wang, Y.-K. Li and C.-Q. Wang, Oxidation and pH responsive nanoparticles based on ferrocene-modified chitosan oligosaccharide for 5-fluorouracil delivery, *Carbohydr. Polym.*, 2014, **114**, 27–35.
49 M. Muraoka, S. L. Gillett and T. W. Bell, Reversible photoinsertion of ferrocene into a hydrophobic semiconductor surface: a chemionic switch, *Angew. Chem., Int. Ed.*, 2002, **41**, 3653–3656.